# Spatial dependence of predictions from image segmentation: a methods to determine appropriate scales for producing land-management information

Jason W. Karl[a,*], Andrea S. Laliberte[a], Albert Rango[a]

[a] Jornada Experimental Range, USDA Agricultural Research Service, New Mexico State University, Las Cruces, NM 88003, USA - (jkarl, alaliber, alrango)@nmsu.edu

**Commission VI, WG IV/4**

**KEY WORDS:** geostatistics, image segmentation, scale, spatial dependence, variogram

**ABSTRACT:**

A challenge in ecological studies is defining scales of observation that correspond to relevant ecological scales for organisms or processes. Image segmentation has been proposed as an alternative to pixel-based methods for scaling remotely-sensed data into ecologically-meaningful units. However, to date, selection of image object sets has been largely subjective. Changing scale of image segmentation affects the variance and spatial dependence (amount and range of spatial autocorrelation) of measured variables, and this information can be used to determine appropriate levels of image segmentation. Our objective was to examine how scaling via image segmentation changes spatial dependence of regression-based predictions of landscape features and to determine if these changes could identify appropriate segmentation levels for a given objective. We segmented an Ikonos image for southern Idaho (USA) into successively coarser scales and evaluated goodness-of-fit and spatial dependence of regression predictions of invasive western juniper (*Juniperus occidentalis*) density. Correlations between juniper density estimates and imagery increased with scale initially, but then decreased as scale became coarser. Scales with highest correlations generally exhibited the most spatial dependence in the regression predictions and residuals. Aggregating original juniper density estimates by image objects changed their spatial dependence, and the point at which spatial dependence began to diverge from the original observations coincided with the highest correlations. Looking at scale effects on spatial dependence of observations may be a simple method for selecting appropriate segmentation levels. The robustness of ecological analyses will increase as methods are devised that remove the subjectivity of selecting scales.

## 1, INTRODUCTION

A significant challenge in ecological studies has been defining scales of observation that correspond to relevant ecological scales for organisms or processes. Scale is a characteristic of a set of observations that controls what patterns can be detected from the observations (Wiens, 1989; Burnett and Blaschke, 2003). Operationally, scale is defined by the smallest observable unit (i.e., grain) and the maximum areal coverage (i.e., extent) of a set of observations (Turner et al., 1989). Because objects smaller than the grain size generally cannot be resolved, and patterns larger than the extent cannot be completely defined, selection of an appropriate scale is important to detecting and describing patterns that result from ecological processes.

Traditionally, scaling of datasets has been accomplished through aggregating observations into successively coarser units of the same size (Wu and Li, 2006). Scaling effects of such methods that use a consistently-shaped support (i.e., analysis unit) include changes in mean and variance (Wu, 2004; Chen and Henebry, 2009) and the existence of scaling domains (Wiens, 1989). However, scaling via consistently-shaped supports can obscure boundaries and can magnify the effects of the modifiable areal unit problem (Dark and Bram, 2007).

Image segmentation has been shown to be an effective method for scaling information such that relevant patterns are preserved and extraneous information (i.e., noise) is removed (Wu, 1999; Burnett and Blaschke, 2003; Hay and Marceau, 2004). This is because image segmentation is a "data-driven" approach to scaling where adjacent observations are merged based on similarity rules. The result of segmentation is a complete tessellation of an area into relatively homogeneous objects of differing shapes and sizes. By varying the degree of similarity needed to merge observations, finer or coarser scale segmentations can be achieved. Karl and Maurer (2010a) reported that higher and more consistent correlations between field and image data were achieved when scaling by image segmentation than by aggregating square pixels.

However, to date, the selection of image object sets to represent landscape patterns has been largely subjective (Wang et al., 2004; Addink et al., 2007) and usually involves trial-and-error for selecting appropriate scales for analysis (Burnett and Blaschke, 2003; Feitosa et al., 2006; Navulur, 2007). However, the accuracy of image-derived products changes with segmentation level (Feitosa et al., 2006; Addink et al., 2007; Karl and Maurer, 2010a), and an optimal scale can be defined as the scale producing the most accurate results for a given objective.

Changes in scale can also affect the magnitude and range of spatial autocorrelation (i.e., spatial dependence) between observations (Fortin and Dale, 2005), but this phenomenon has

* Corresponding author. Email: jkarl@nmsu.edu, phone: 575-646-7015.

not been studied extensively in object-based scaling. Karl and Maurer (2010b) showed that optimal object-based scales for predicting attributes of a semi-desert landscape minimized spatial autocorrelation of regression residuals. However, they also demonstrated that geostatistical techniques that could account for this residual spatial autocorrelation could yield predictions from scales finer than optimal that were about as accurate as predictions from the optimal scale. This suggests that spatial dependence of image objects relative to that of field observations may be an important trait in selecting object-segmentation scales for analyses.

Our objective was to examine how scaling via image segmentation changes the spatial dependence of regression-based predictions of landscape features. Specifically we were interested in whether or not changes in observed spatial dependence of original measurements or regression predictions and residuals could be used to identify optimal (or near-optimal) scales of segmentation.

## 2. STUDY AREA

This study was conducted in the 47,700-ha Castle Creek area in southwestern Idaho, USA (116.5ºW, 42.7ºN, Figure 1). The Castle Creek landscape, a semi-arid shrub-steppe environment receiving on average between 26.7mm and 57.0mm of precipitation annually, is typified by rolling hills and low plateaus. Vegetation in the area is a mosaic of mountain mahogany (*Cercocarpus ledifolius*) western juniper (*Juniperus occidentalis*) and different sagebrush (*Artemisia tridentata* ssp. *tridentata*, *Artemisia tridentata* ssp. *vaseyana*, *Artemisia arbuscula*) communities with native bunchgrass in the understory.

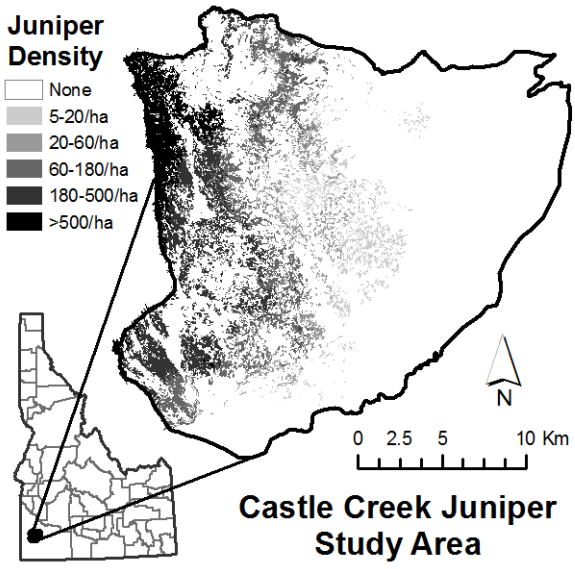


Figure 1. Estimated distribution and density of juniper in the Castle Creek study area in southern Idaho, USA.

A century of fire suppression in the western United States has led to many ecological changes by disrupting the frequency of a coarse-scale natural process. In southern Idaho, one effect of fire suppression has been the expansion of western juniper beyond its historic range into previously unoccupied habitats. Juniper is a long-lived species and thick layers of litter accumulate under larger trees that suppress the growth of other plants. This expansion of juniper has led to a decrease in the value of rangelands for livestock or as habitat for wildlife species like sage grouse (*Centrocercus urophasianus*) as the native shrubs, grasses, and forbs are lost. The U.S. Bureau of Land Management (BLM), the majority land manager in the Castle Creek area has identified the Castle Creek area as a priority landscape for addressing the expansion of juniper and restoring native sagebrush-steppe communities.

In the Castle Creek area, juniper was historically restricted to places that typically did not burn like rocky outcrops, cooler ridges and mountain tops, and isolated plateaus. Over time, however, the distribution of juniper in Castle Creek area has expanded from its limited distribution in the western portion of the study area to cover much of the western half of the study area.

## 3. METHODS

We followed a similar method to Karl and Maurer (2010b) where a satellite image was segmented multiple times to achieve realizations of different scales. At each scale, estimates of juniper density were correlated via regression with pixel means and standard deviations for each image object and the spatial dependence of regression predictions and residuals was compared.

### 3.1 Imagery Acquisition and Processing

We acquired a multispectral Ikonos image for the Castle Creek area on July 31, 2008. The image was radiometrically corrected and orthorectified by GeoEye (http://www.geoeye.com) and had a ground resolution of 4 m. The image had four spectral bands: blue (445 to 516 nm), green (506 to 595 nm), red (632 to 698 nm) and near-infrared (757 to 853 nm). The image was atmospherically corrected using a dark-object subtraction method (Chavez, 1996), and the 11-bit digital numbers for each pixel were converted to top-of-atmosphere reflectance.

Because image segmentation is sensitive to correlations between image bands (see Navulur, 2007), we applied a tasselled-cap transformation to the Ikonos image using the coefficients developed by Horne (2003) for the Ikonos sensor. The tasselled-cap transformation is a linear combination of the original image bands to create a new set of bands with specific interpretations. Tasselled-cap band one is interpreted as brightness of the image. Band two is interpreted as greenness and correlates highly with other vegetation indexes. Band 3 is interpreted as "wetness." The fourth tasselled-cap band contains much noise and is generally discarded. We used the first three tasselled-cap bands from the Ikonos image as inputs for the image segmentation and subsequent statistical analyses.

### 3.2 Image Segmentations

Segmentation of the tasselled-cap transformed Ikonos image into object sets of different scales was accomplished with Definiens Developer 7.0 using the multi-scale resolution segmentation (MRS) algorithm described by Baatz and Schäpe (2000; see also Burnett and Blaschke, 2003). The MRS algorithm works by merging adjacent pixels in the first iteration and objects in later iterations and evaluating the increase in local heterogeneity. If after merging the local heterogeneity is below a set threshold, the merged objects are kept, otherwise, the merge is abandoned and a different combination of objects is tried. This procedure continues until all possible merges below the threshold are made. The heterogeneity threshold is set via a user-specified scale parameter ($p_s$). By increasing $p_s$,

greater heterogeneity is allowed within image objects and, in general, the size of the objects increases. Objects that are very distinct from their surroundings, however, will tend to be maintained as independent image objects while the objects around them increase in size until a point is reached where they are dissolved into the adjacent objects (Karl and Maurer, 2010a).

We segmented the tasselled-cap transformed Ikonos image for the Castle Creek area 14 times to create a set of image segmentations that became increasingly coarser in scale. For each successive segmentation, we increased $p_s$ by a set amount (Table 1). The image objects for each segmentation level were attributed with the mean and standard deviation of the pixels within each image object for all the tasselled-cap bands and then exported for statistical analysis.

| Scale Para. ($p_s$) | Number of Objects | Median Area (ha) | Minimum Area (ha) | Maximum Area (ha) |
|---|---|---|---|---|
| 20 | 115792 | 0.434 | 0.002 | 14.691 |
| 30 | 51,352 | 0.990 | 0.006 | 15.941 |
| 40 | 29,392 | 1.712 | 0.010 | 29.475 |
| 50 | 19,193 | 2.618 | 0.027 | 43.760 |
| 60 | 13,506 | 3.722 | 0.027 | 63.138 |
| 70 | 9,988 | 5.000 | 0.037 | 91.333 |
| 80 | 7,686 | 6.461 | 0.077 | 171.789 |
| 90 | 6,064 | 8.010 | 0.077 | 171.789 |
| 100 | 4,880 | 9.890 | 0.077 | 214.902 |
| 110 | 4,031 | 11.799 | 0.112 | 246.192 |
| 120 | 3,374 | 14.139 | 0.126 | 246.192 |
| 130 | 2,890 | 16.750 | 0.205 | 246.192 |
| 140 | 2,501 | 18.995 | 0.226 | 314.798 |
| 150 | 2,184 | 21.518 | 0.226 | 314.798 |

Table 1. Statistics for the successively coarser segmentations

### 3.3 Estimating Juniper Density

The density of juniper in the Castle Creek area was estimated from 1m-resolution aerial photographs. We used aerial photographs collected by the U.S. Department of Agriculture's National Aerial Imagery Program (NAIP) on September 14, 2009. Because juniper is a slow-growing, long lived species and no wildfires or juniper management actions occurred between the dates of the Ikonos and NAIP image acquisition, we concluded that any difference between image dates would not significantly affect our results.

Sample locations were generated for 221 points within the study area using two different sampling schemes. A previous field project had sampled 126 randomly-selected points within the area. We supplemented these locations with an additional 95 points placed on a regular grid with 2km spacing between points. This dual sampling scheme was used to improve the ability to measure and model spatial dependence in the juniper density estimates.

A circle of 55m radius was placed around each sample point. This size of circle was selected because it corresponds to a standard plot size for shrubland sampling. Within each circle, the number of juniper visible at a scale of 1:2000 was counted. The number of juniper was divided by the plot area (0.95 ha) to get the density of juniper per hectare.

### 3.4 Associating Juniper Density with Image Objects

Statistical analyses followed the methods described in Karl and Maurer (2010b) and were performed in R version 2.10.1 using the *nlme* (Pinheiro and Bates, 2000) and *gstat* (Pebesma, 2004) packages for generalized least-squares (GLS) regression and variogram estimation and modelling, respectively. All variables were transformed using log or square-root transformations as necessary to meet normality assumptions of linear regression.

The presence of a geographic trend in data obscures the ability to detect spatial autocorrelation between observations. In the Castle Creek area, however, there is a strong moisture gradient from east to west that influences spectral reflectance as well as the distribution and density of juniper (Figure 1). This trend was removed by regressing the image object information at each scale and the juniper density estimates by their X and Y coordinate values (and including an X/Y interaction). The residuals from these regressions represent geographically de-trended data which were used throughout the rest of the study.

To assess the spatial dependence of the juniper density estimates, we constructed a semi-variogram between all pairs of observations following Fortin and Dale (2005). We fit an omni-directional, spherical variogram model to the empirical variogram. The variogram was characterized by its nugget (i.e., variance that cannot be explained by distance between observations - including measurement error), sill (i.e., total observed semivariance), and range (i.e., distance at which two observations can be considered independent)(see Fortin and Dale, 2005). The nugget-to-sill ratio (NSR) was used as a measure of the proportion of total observed variation that could not be explained by the observed spatial dependence of the variable.

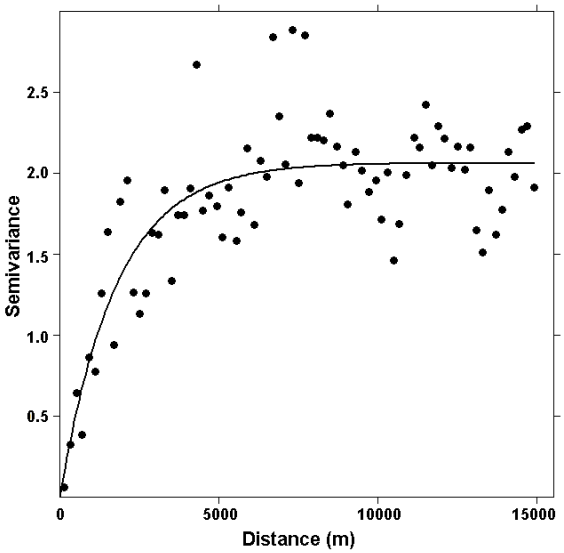


Figure 2. Empirical variogram (dots) and variogram model (line) of the de-trended juniper density estimates in the Castle Creek area. The juniper-density nugget-to-sill ratio was 0.1457.

To test how scale affected the relationship between the juniper density estimates and the image object information, we used generalized least-squares (GLS) regression and analyzed the spatial dependence of the GLS model predictions and residuals via variogram modelling. The first step at each segmentation level was to select the image objects that contained one or more juniper density estimates. Coordinate values were determined

| $p_s$ | R | GLS Regression Prediction | | | | GLS Regression Residual | | | |
|---|---|---|---|---|---|---|---|---|---|
| | | Nugget | Sill | NSR | Range | Nugget | Sill | NSR | Range |
| 20 | 0.6786 | 0.4722 | 0.6501 | 0.7263 | 1,320 | 0.6299 | 1.1230 | 0.5609 | 1,320 |
| 30 | 0.7092 | 0.2601 | 0.7633 | 0.3407 | 1,903 | 0.2348 | 1.0080 | 0.2329 | 2,661 |
| 40 | 0.7123 | 0.1093 | 0.8115 | 0.1347 | 1,458 | 0.3084 | 1.0036 | 0.3073 | 2,558 |
| 50 | 0.7280 | 0.1814 | 0.8731 | 0.2077 | 1,998 | 0.1964 | 0.9592 | 0.2048 | 2,714 |
| 60 | 0.7293 | 0.1074 | 0.8391 | 0.1280 | 1,621 | 0.3133 | 0.9672 | 0.3240 | 3,104 |
| 70 | 0.7182 | 0.2191 | 0.8436 | 0.2597 | 1,902 | 0.3173 | 1.0385 | 0.3055 | 3,324 |
| 80 | 0.6952 | 0.1231 | 0.8028 | 0.1533 | 1,833 | 0.4745 | 1.1198 | 0.4238 | 4,741 |
| 90 | 0.7006 | 0.1809 | 0.8394 | 0.2155 | 1,883 | 0.3367 | 1.0575 | 0.3184 | 2,999 |
| 100 | 0.6816 | 0.1109 | 0.7885 | 0.1406 | 1,958 | 0.4792 | 1.1431 | 0.4192 | 5,532 |
| 110 | 0.6833 | 0.3774 | 0.7919 | 0.4766 | 2,197 | 0.4590 | 1.1199 | 0.4099 | 4,864 |
| 120 | 0.6675 | 0.4433 | 0.7323 | 0.6054 | 1,890 | 0.5087 | 1.1747 | 0.4331 | 5,392 |
| 130 | 0.6714 | 0.7145 | 0.7376 | 0.9687 | 2,162 | 0.6114 | 1.1543 | 0.5297 | 6,146 |
| 140 | 0.6492 | 0.5862 | 0.6748 | 0.8687 | 2,023 | 0.6379 | 1.2161 | 0.5245 | 6,523 |
| 150 | 0.6294 | 0.5753 | 0.6294 | 0.9139 | 2,516 | 0.4474 | 1.2772 | 0.3503 | 4,646 |

Table 2. Correlation (R) between juniper density estimates and GLS-regression predictions of juniper density and variogram characteristics of GLS-model predictions and residuals at each segmentation level ($p_s$).

for the geometric center of each image object. When more than one juniper density estimate fell within an image object, the estimates were averaged to provide a single juniper density estimate per image object. We used this method to avoid artificially inflating sample sizes for coarser scales and because it was akin to taking multiple samples within an object.

The next step was, for each $p_s$, to use GLS regression to establish the relationship between the juniper density estimates and the image object values. We used GLS to incorporate spatial covariance between samples (Bailey and Gatrell, 1995). We included all 6 image-band measures (i.e., mean and standard deviation of pixels per object for the three tasselled-cap bands) in an initial regression model. A backward variable-selection technique was used to select the most parsimonious model by comparing Akaike's information criterion (AIC values (Burnham and Anderson, 2002). For each $p_s$ we recorded the correlation between the final model and the original estimates as a measure of the association between the juniper density estimates and the image objects at that scale. Finally, we constructed variograms and variogram models for the GLS regression predictions and residuals for each $p_s$.

Ideally, a method could be defined to identify optimal scales without the need to conduct regressions on many different segmentation levels. In light of this, and because of the relationship between the regression NSR and overall correlation between juniper density and image objects, we further explored the effects of aggregating the original juniper density estimate points by image objects at different $p_s$. Variograms and variogram models were constructed from the aggregated juniper density points at each $p_s$.

## 4. RESULTS

The de-trended juniper density estimates showed strong spatial autocorrelation (Figure 2). The variogram of the juniper density estimates had a range of 4,968m, and a nugget and sill of 0.2968 and 2.0365, respectively. The NSR for juniper density estimates was 0.1457 - indicating strong spatial dependence.

Correlation between juniper density and the image objects increased with segmentation level until $p_s$ = 60, whereafter it steadily decreased (Table 2, Figure 3). Generally, the scales with the highest juniper-estimate to image correlations also had the lowest NSR for both the GLS predictions and residuals (Figure 4). Regression between correlation coefficients at each $p_s$ and the variogram NSR for that scale gave an $R^2$ of 0.6748 (p=0.0003) and 0.4053 (p=0.0144) for the GLS predictions and residuals, respectively. For variogram range, similarly-derived $R^2$ values were 0.2152 (p=0.0539) and 0.3288 (p=0.0188) for the GLS predictions and residuals, respectively.

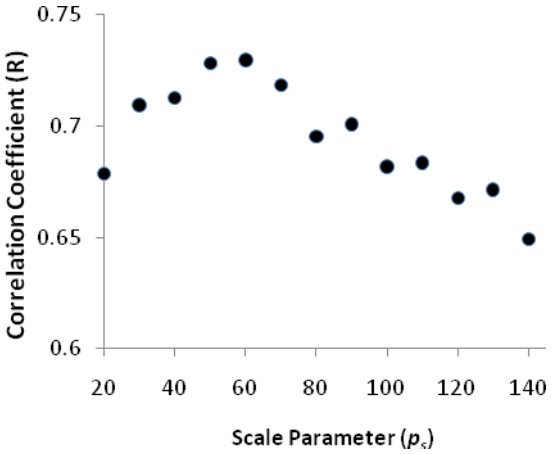


Figure 3. Changes in correlation between juniper density estimates and predictions of juniper density from the GLS-regression models.

Aggregation of the original juniper density points by different scales of image objects altered their spatial dependence. At fine scales ($p_s$ <= 60), there was little departure from the spatial dependence of the original observations (Figure 5) because most objects contained only one point. As more observations were averaged into single image objects with increasing $p_s$, the range and NSR of the juniper density points began to diverge from the original points. The point at which this divergence began coincided with the $p_s$ that yielded the highest juniper-density to field correlation ($p_s$=60).

## 5. DISCUSSION

Our results support previous research that suggests that segmentation scales can be defined that maximize the correlation between field and image measurements (Feitosa et al., 2006; Addink et al., 2007). Furthermore, our results support the idea that changes in spatial dependence can be used to identify appropriate ranges of scales (Karl and Maurer, 2010b). Karl and Maurer (2010b) suggested that segmentation scales with a NSR and range that closely matched the field observations would be optimal because segmentation can preserve variance between objects in such a way that the variance structure of the original observations is maintained. Our results in Figure 5 support this theory. However our results from Figure 4, namely that those scales with the highest spatial dependence (i.e., lowest NSR) performed best, do not. This disparity may be related to scales of the ecological processes affecting the distribution of juniper.

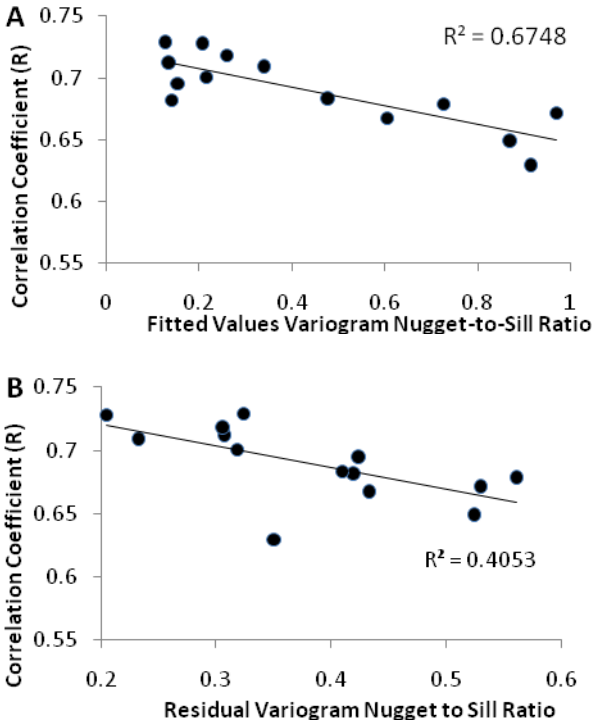


Figure 4. Correlation between juniper density estimates and predictions from GLS-regression models was related to the spatial dependence of the predictions (A) and the model residuals (B). Low nugget-to-sill ratios in both the model predictions and residuals (signifying large spatial dependence) yielded the highest correlations.

Factors important to describing the distribution and density of juniper in Castle Creek not accounted for by the image information may be obscuring the expected pattern. Spatial dependence in regression model residuals is the result of unexplained variability that is related to distance (Bailey and Gatrell, 1995). In the Castle Creek area, juniper density exhibited much more, and shorter range spatial dependence than did bare ground that Karl and Maurer (2010b) examined. Some portion of the juniper spatial dependence may be related to factors other than those directly recorded by the Ikonos sensor (e.g., aspect, soil type, fire and management history). If this is the case, incorporation of these additional factors would increase spatial dependence for the model predictions and reduce it for model residuals. But the influence of these covariates might not be the same at all segmentation scales. For instance, a fine-scale variable like aspect is likely to be strongly associated with with juniper density at fine segmentation levels where each segment is more likely to contain a single aspect than at coarse segmentation levels where multiple aspects will be combined per image object. This could produce the expected pattern of spatial dependence relative to optimal segmentation levels.

A more reliable technique for identifying ranges of appropriate scales may be to look at changes in spatial dependence of the original observations under different segmentation scales. This has the advantage that it can be easily done and does not require running repeated regressions against multiple scales of image objects and examining the correlations. As original observations are aggregated into coarser scales, spatial dependence begins to shift toward larger NSR (i.e., less spatial dependence) and longer ranges (Figure 5). Initially, this change is minor as most image objects still contain only one observation point. Eventually, however, the scale becomes coarse enough that many points are being aggregated, and the measured spatial dependence shifts significantly from that of the original observations. Because correlation between field and image information for image segmentation tends to increase with scale (Karl and Maurer, 2010a), the optimal scale for a variable may be the point just before deviation from field measurements becomes large (e.g., $p_s$=60 for juniper in Castle Creek). While image segmentation scales below this level may be sub-optimal, they could still be considered appropriate because use of geostatistical techniques like regression kriging (see Hengl et al., 2004) can yield results nearly as accurate (Karl and Maurer, 2010b).

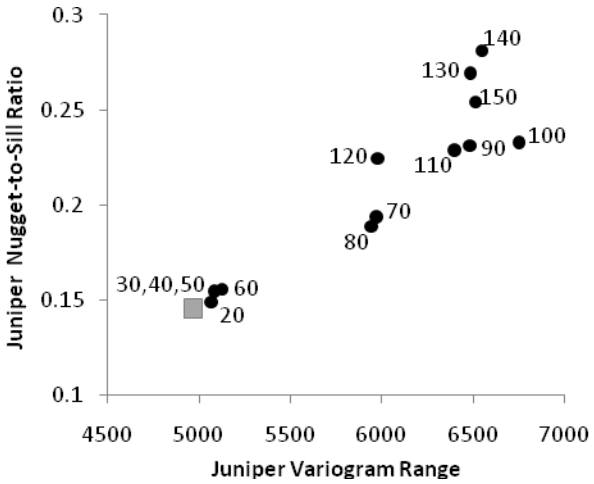


Figure 5. Plot of variogram range versus nugget-to-sill ratio (NSR) for the original juniper density estimate points aggregated by different scales of image objects. Segmentation levels with range and NSR closest to the original points (gray square) had the highest correlations between juniper density estimates and GLS-regression predictions. Point labels correspond to the segmentation scale parameter ($p_s$).

## 6. CONCLUSION

This study supports a growing body of literature on the importance of selecting appropriate scales for analysis. The contribution of this study is that it 1) reinforces the assertion that scaling via image segmentation affects spatial dependence of observations and predictions, and 2) describes a simple

method for evaluating the appropriateness of different scales by looking at the effect of a scale on the spatial dependence of a set of observations.

In order to understand the relationships between patterns and processes across landscapes, it is necessary to collapse information into units of different scale to remove unnecessary information and extract patterns of interest (Wu, 1999; Burnett and Blaschke, 2003). Image segmentation has shown promise as a way to scale information for ecological analyses, but more work is needed to understand how different segmentation scales affect information content and the quality of predictions, and ultimately to develop reliable methods for selecting appropriate scales for analysis. The robustness of landscape analyses will increase as methods are devised that remove the subjectivity with which observational scales are defined and selected.

## REFERENCES

Addink, E. A., S. M. de Jong, and E. J. Pebesma. 2007. The importance of scale in object-based mapping of vegetation parameters with hyperspectral imagery. Photogrammetric Engineering and Remote Sensing 73:905-912.

Baatz, M., and A. Schäpe. 2000. Multiresolution segmentation - an optimization approach for high quality multi-scale image segmentation. Pages 12-23 *in* J. Strobl, T. Blaschke, and G. Griesebner, editors. Angewandte Geographische Informationsverarbeitung XII. Wichmann-Verlag, Heidelberg.

Bailey, T. C., and A. C. Gatrell. 1995. Interactive spatial data analysis. Addison-Wesley.

Burnett, C., and T. Blaschke. 2003. A multi-scale segmentation/object relationship modelling methodology for landscape analysis. Ecological Modeling 168:233-249.

Burnham, K. P., and D. R. Anderson. 2002. Model selection and multimodel inference: a practical information-theoretic approach, second edition. Springer, New York.

Chavez, P. S., Jr. 1996. Image-based atmospheric corrections - revisited and improved. Photogrammetric Engineering and Remote Sensing 62:1025-1036.

Chen, W., and G. M. Henebry. 2009. Change of spatial information under rescaling: a case study using multi-resolution image series. Journal of Photogrammetry and Remote Sensing 64: 592-597.

Dark, S. J., and D. Bram. 2007. The modifiable areal unit problem (MAUP) in physical geography. Progress in Physical Geography 31:471-479.

Feitosa, R. Q., G. A. O. P. Costa, T. B. Cazes, and B. Feijo. 2006. A genetic approach for the automatic adaption of segmentation parameters.*in* First International Conference on Object-based Image Analysis. Salzburg University, Salzburg, Austria.

Fortin, M. J., and M. Dale. 2005. Spatial analysis: a guide for ecologists. Cambridge University Press, Cambridge, UK.

Hay, G. J., and D. J. Marceau. 2004. Multiscale object-specific analysis (MOSA): an integrative approach for multiscale landscape analysis.*in* S. M. de Jong and F. D. van der Meer, editors. Remote Sensing and Digital Image Analysis: including the spatial domain. Kluwer Academic Publishers, Dordecht, Germany.

Hengl, T., G. B. M. Heuvelink, and A. Stein. 2004. A generic framework for spatial prediction of soil variables based on regression-kriging. Geoderma 120:75-93.

Horne, J. H. 2003. A tasseled cap transformation for IKONOS images.*in* ASPRS 2003 Annual Conference Proceedings. ASPRS.

Karl, J. W., and B. A. Maurer. 2010a. Multivariate correlations between imagery and field measurements across scales: comparing pixel aggregation and image segmentation. Landscape Ecology 24:591-605.

Karl, J. W., and B. A. Maurer. 2010b. Spatial dependence of predictions from image segmentation: a variogram-based method to determine appropriate scales for producing land-management informatino. Ecological Informatics. *In Press*, Availble online March 1, 2010.

Navulur, K. 2007. Multi-spectral image analysis using the object-oriented paradigm. CRC Press, Taylor and Francis Group, LLC, Boca Raton, FL.

Pebesma, E. J. 2004. Multivariable geostatistics in S: the gstat package. Computers & Geosciences 30:683-691.

Pinheiro, J. C., and D. M. Bates. 2000. Mixed-effects models in S and S-PLUS. Springer Verlag, New York, NY.

Turner, M. G., R. V. O'Neill, R. H. Gardner, and B. T. Milne. 1989. Effects of changing spatial scale on the analysis of landscape pattern. Landscape Ecology 3:153-162.

Wang, L., W. P. Sousa, and P. Gong. 2004. Integration of object-based and pixel-based classification for mapping mangroves with IKONOS imagery. Internation Journal of Remote Sensing 25:5655-5668.

Wiens, J. A. 1989. Spatial scaling in ecology. Functional Ecology 3:385-397.

Wu, J. 1999. Hierarchy and scaling: extrapolating information along a scaling ladder. Canadian Journal of Remote Sensing 25:367-380.

Wu, J. 2004. Effects of changing scale on landscape pattern analysis: scaling relations. Landscape Ecology 19:125-138.

Wu, J., and H. Li. 2006. Concepts of scale and scaling. Pages 3-15 *in* J. Wu, K. B. Jones, H. Li, and O. L. Loucks, editors. Scaling and Uncertainty Analysis in Ecology: Methods and Applications. Springer, Dordrecht, the Netherlands.

## ACKNOWLEDGMENTS

This work was supported, in part, by the Idaho Chapter of The Nature Conservancy and the M.J. Murdock Charitable Trust.